Thin Solid Films 734 (2021) 138860

Contents lists available at ScienceDirect

Thin Solid Films

journal homepage: www.elsevier.com/locate/tsf

Electrochemical deposition of indium into oxidized and unoxidized porous silicon

Nikita Grevtsov [a,*], Eugene Chubenko [a], Vitaly Bondarenko [a], Ilya Gavrilin [b], Alexey Dronov [b], Sergey Gavrilov [b]

[a] Belarusian State University of Informatics and Radioelectronics, P. Brovki str. 6, Minsk 220013, Belarus
[b] National Research University of Electronic Technology, Zelenograd, Moscow, Russia

ARTICLE INFO

Keywords:
Porous silicon
Fusible metals
Indium
Electrochemical deposition
Oxidation

ABSTRACT

Various cases of electrochemical deposition of indium into oxidized and unoxidized mesoporous silicon were investigated and subsequently compared. The results would suggest that both thermal and chemical oxidation of porous silicon cause the metal particles being deposited into its pores to shift deeper along the pore channels due to the latter's topmost areas being oxidized the most and therefore becoming significantly less conductive and more easily wettable by both the deposition solution and indium itself upon its subsequent thermal processing. However, oxidation becomes less effective as the thickness of the porous layer is increased due to the gradually escalating effect of reduced conductivity at the pore tips. Potentially, porous silicon layers with indium particles localized in the bottommost parts of the pore channels could be used to form germanium nanostructures inside the pores, allowing subsequent creation of Ge-Si alloys by utilizing the electrochemical liquid-liquid-solid approach.

1. Introduction

Up to this point, a variety of approaches to depositing fusible metals and alloys with low temperature melting points (less than 233 °C – tin melting point) onto conductive substrates have been thoroughly researched, including but not limited to chemical vapor deposition, electrochemical deposition techniques involving photolithography and other forms of masking, as well as miscellaneous electrodeposition methods [1–4]. However, fusible metal deposition onto porous wafers – namely, porous silicon (*PS*) – is substantially less explored in literature, with only a few works delving into such a possibility. It has been shown that indium can be electrodeposited onto PS using a solution containing indium chloride [5]. Another reproducible method to deposit indium particles into porous layers was summarized by Ito [et al.] [6], albeit the metal's distribution throughout the pore channels was not elaborated upon. The deposition method (specifically, the solution composition) chosen in the present work is based on the above-mentioned research.

The prime interest of forming indium particles on either monocrystalline or PS wafers is the prospect of using them as a structural basis to form germanium nanostructures and Ge-Si alloys via the *electrochemical liquid-liquid-solid* growth process (*ec-LLS*) [7]. This approach involves using fusible metals as a growth medium for germanium nanostructures [8]. At the same time, the metal particles serve as microscopic cathodes, providing electrons for the forming germanium deposits [9].

It should be noted that the effectiveness of performing ec-LLS on porous media has not yet been assessed. We presume that if such a technique was performed on a PS substrate with fusible metal particles uniformly localized in the bottommost parts of the pore channels, a silicon matrix continuously filled with germanium wires could be acquired. The latter in turn could be subsequently annealed to produce silicon-germanium alloys widely known for their thermoelectric capabilities. Apart from its *ec-LLS*-related applications, the proposed indium plating method could also potentially be used to form conductive electrical contacts to PS and monocrystalline silicon [10].

Here, in our research, we have studied the process of electrochemical deposition of indium into as-prepared (unoxidized) and additionally modified (partially oxidized) mesoporous silicon from an aqueous solution to obtain structures suitable for subsequent *ec-LLS* deposition of germanium.

* Corresponding author.
E-mail address: hrautsou@gmail.com (N. Grevtsov).

https://doi.org/10.1016/j.tsf.2021.138860
Received 2 December 2020; Received in revised form 26 May 2021; Accepted 25 July 2021
Available online 29 July 2021

2. Experimental details

Electrochemical processing was carried out in a two electrode electrochemical cell (Fig. 1) utilizing a Metrohm Autolab PGSTAT302N potentiostat as a current source.

Porous silicon was formed by anodizing 460 μm-thick Sb-doped (100)-oriented monocrystalline silicon wafers with a bulk resistivity of 0.01 Ohm-cm in galvanostatic mode at a current density of 70 mA/cm^2 using a solution consisting of hydrofluoric acid (HF, analytical grade, 45 wt. % in H_2O), deionized water (H_2O, resistivity 17 MOhm cm) and isopropyl alcohol (C_3H_7OH, analytical grade, $\geq$ 99.8%) mixed in a volume ratio of 1:3:1. Negative potential was applied to the counter-electrode (platinum wire) and positive to the working electrode (silicon wafer) for the anodization process. The area of the working electrode exposed to the deposition solution was 3 cm^2.

We have speculated that oxidation of PS prior to electrochemical deposition of indium could potentially lead to the latter's preferential conglomeration in the lowermost areas of the pore channels due to those areas being oxidized least. Two oxidation methods were selected in order to compare the according indium deposition results with those obtained on unoxidized PS: (1) chemical oxidation in nitric acid (HNO_3, analytical grade, 50 wt. % in H_2O) and (2) thermal oxidation at 300 °C. For chemical oxidation, PS substrates were dipped in HNO_3 immediately after their formation and kept there for 30 min. Thermal oxidation was carried out with a laboratory thermal heater in the air atmosphere for the same amount of time (30 min).

In each case indium was deposited into PS electrochemically from a solution containing indium sulfate ($In_2(SO_4)_3$, Fluka AG, $\geq$ 98.0%), deionized water and sodium sulfate (Na_2SO_4, analytical grade, $\geq$ 99.0%) mixed in a 6:300:1 mass ratio. The deposition process was carried out at two different current densities (0.5 and 5 mA/cm^2) and different deposition times (t_{dep}) ranging from 600 to 1800 s using the same two-electrode electrochemical cell, with the exception of the electrode polarity being reversed. In addition to that, to avoid the solution's depletion, an indium wire was utilized as a counter-electrode. The samples were immersed in the deposition solution for 30 min prior to applying the current in order to evenly distribute the electrolyte throughout the porous media.

General morphology study and elemental analysis of the samples were performed using a Hitachi S-4800 scanning electron microscope (SEM) (Japan) equipped with a Bruker QUANTAX 200 energy-dispersive X-ray analyzer (EDS) (Germany), acquiring element spatial distribution maps overlaid over their corresponding SEM images. For distribution comparison, concentration profiles were obtained by scanning each sample diagonally across the porous layer.

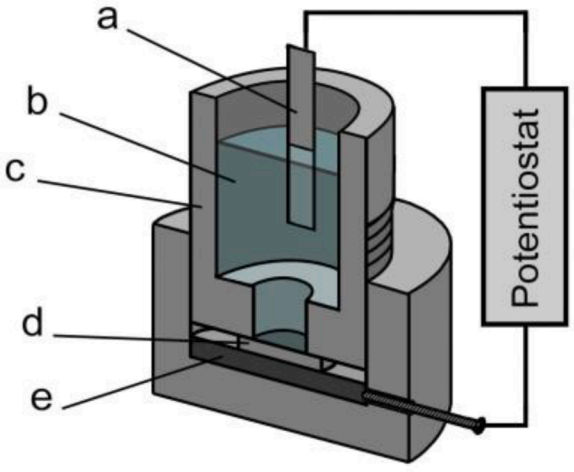

Fig. 1. Schematic overview of the two-electrode electrochemical cell setup used for the anodization of silicon and electrodeposition of indium: (a) counter-electrode, (b) anodization/deposition solution, (c) polytetrafluoroethylene body, (d) sample (working electrode), (e) graphite electrode providing electrical contact to sample.

It should be noted that this particular method of elemental analysis relies on acquiring the X-ray spectra from a volume of around 0.5 μm^3. Since the structures in question generally fall below this size threshold, the data obtained via this method (EDS concentration profiles and EDS maps) can be perceived as average throughout said volume and are therefore expressed in arbitrary units. As the conditions of the EDS analysis remained unchanged for all the samples discussed below, we consider this approach reasonable due to only using these concentration values as means of comparison.

3. Experimental results

3.1. Effect of different oxidation methods and PS layer depths

In this section, samples obtained using different oxidation methods and porous layer thicknesses are compared to each other in terms of the structural characteristics of indium particles deposited into them in the same processing regimes.

The thickness of the PS layer formed by anodization is directly dependent on the anodization time (t_{an}) [11]. Cross-section SEM images of samples obtained at different processing times (Fig. 2) allow us to determine that the average thicknesses of PS layers are 1.6 μm for t_{an} = 30 s, 5.5 μm for t_{an} = 120 s and 12 μm for t_{an} = 240 s. As the same current density was maintained, pore diameters remained roughly the same for all samples, varying from 30 to 140 nm with an average of 80 nm.

Indium deposition was carried out for 10 min at a current density of 0.5 mA/cm^2 for all the samples listed in this section. The EDS maps adjacent to SEM images display the approximate distribution of indium particles throughout the pore channels, with the corresponding relative concentration profiles based on the same EDS data positioned below. Throughout the latter, the 0% mark on the horizontal axis corresponds to the upper edge of the porous layer, while the 100% mark signifies the interface between porous and monocrystalline silicon. It should be noted that indium concentration does not reach zero at the PS/monocrystalline silicon border because the diameter of X-ray scanning beam has a finite size, leading to dispersion and averaging of EDS data (as described in the previous section).

Vertical conglomerations of indium particles can be seen filling pores in a selective manner. The metal filaments can be identified as brighter areas on the SEM images, more easily distinguished on the accompanying EDS maps. It should be noted that the highest concentration of indium is typically observed in the central part of the porous layer. According to the EDS-based concentration profiles measured along the pore depth (Fig. 2), the distribution of indium remains very similar for both unoxidized and oxidized samples of all thicknesses. However, in the cases of thinner porous silicon layers (1.6 μm and 5.5 μm) the overall amount of indium deposited in chemically and thermally oxidized PS is notably higher than that in unoxidized samples.

3.2. Effect of thermal treatment of deposited metal particles

To improve the metal's distribution throughout the pore channels, samples obtained at different t_{an}, t_{dep} and oxidation modes were subsequently subjected to thermal annealing at 200 °C in vacuum over the course of 15 min in order to melt the deposited indium particles. A comparison of SEM images and EDS maps of these samples and the corresponding concentration profiles are presented in Fig. 3.

Lesser anodization times of t_{an} = 15 s, and t_{an} = 30 s were utilized in this experiment, acquiring 0.8 and 1.6 μm-thick porous layers, accordingly, with pore diameters ranging from 25 to 130 nm in both cases. The concentration profiles and EDS maps display a notably prevalent concentration of indium on the surface and in the subsurface areas of unoxidized PS layers that rapidly decreases with pore depth in a nearly

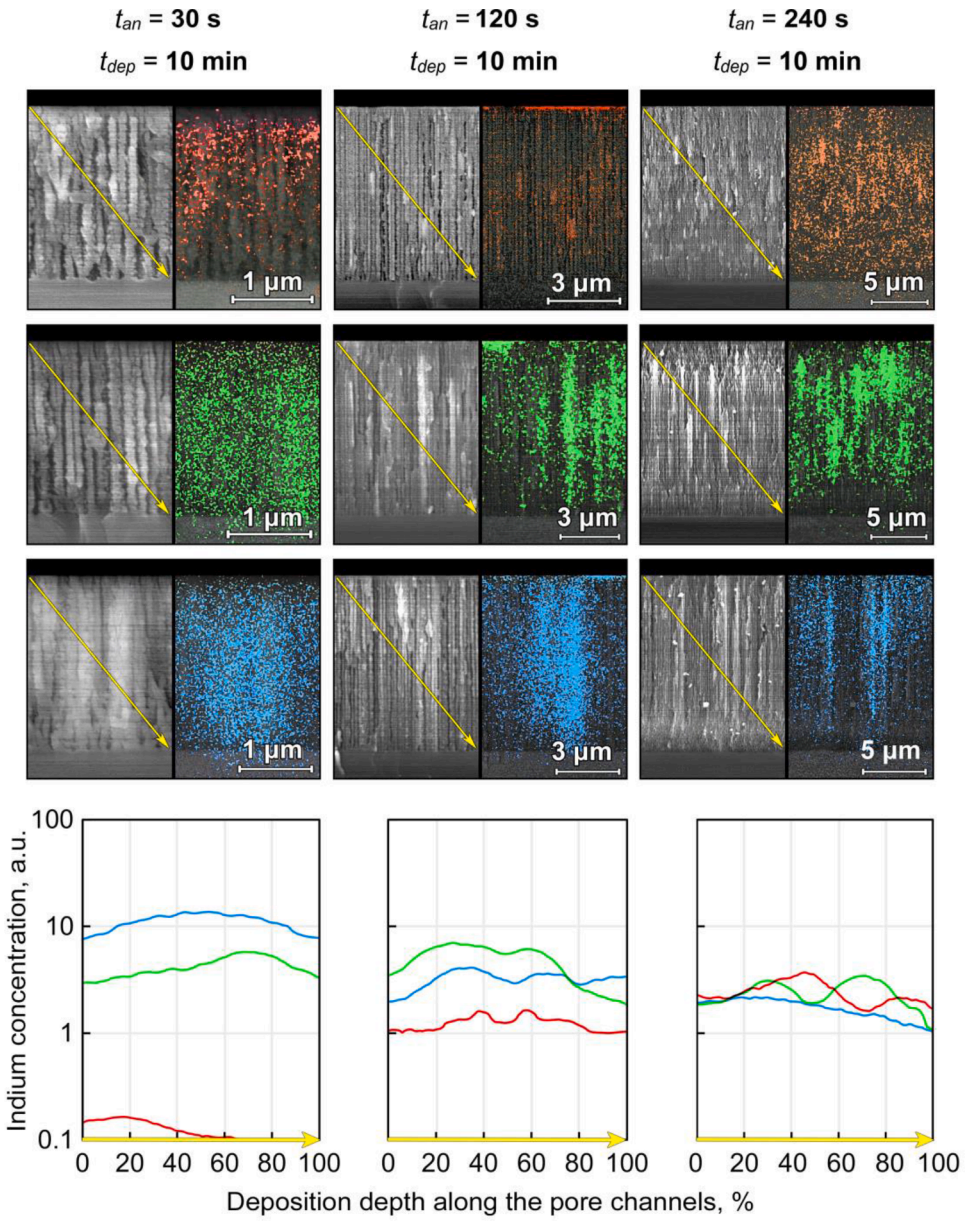

Fig. 2. Cross-section SEM images of indium-plated PS samples obtained at different anodization times and pre-deposition oxidation modes (left side of each image) and corresponding EDS maps (right side) showcasing indium distribution (colored areas): and corresponding EDS-based concentration profiles of indium deposited into (red) unoxidized, (green) chemically oxidized and (blue) thermally oxidized PS layers formed at three different anodization times (t_{an}). Yellow arrows indicate the position and direction of EDS scans.

linear fashion. In contrast to that, indium concentration in oxidized samples is noticeably more uniform, implying a crucial difference in the thermal treatment's effect. It should be noted that a substantially thick layer of indium was present on the surface for most of the experimental samples listed, but the locations of SEM and EDS analysis were picked to specifically focus on the pore filling aspect and eliminate the input of surface deposits into the EDS signal.

3.3. Effect of pore size and current density

In order to comprehend the effect of pore size on indium deposition into PS layers we performed a statistical analysis of lateral pore sizes using surface SEM images of chemically and thermally oxidized samples presented in Fig. 4. The subsurface layer of these particular samples was removed by ion milling, allowing to examine the degree of pore filling at about 1 um from the surface of the porous porous layer.

Despite the number of indium-filled pores appearing to be considerably larger for unoxidized PS, any valid assertions of the pore filling factor would be impossible to conduct based on these images alone due to the indium particles being scattered all throughout the porous layer, making them unlikely to be visible all at once at the same height. However, the results of the pore size distribution analysis for each of the images (Fig. 5) would indicate that indium particles reside in pores with larger lateral sizes, as opposed to smaller pores that tend to only have occasional particles on their side-walls.

To further investigate the pore filling mechanism, various ways of maximizing the number of pores filled were evaluated, such as increasing the pore diameter and the deposition current. Pores in mesoporous silicon tend to have a bottle-like shape with narrow "necks" near the surface [11]. The thickness of this subsurface microporous subsurface layer is usually about 100 nm [12]. In order to remove it, we used the dry process of ion sputtering. This approach allows to open up a more uniform underlying layer of PS possessing greater pore diameters. Our second approach to increasing the lateral pore sizes consisted of applying a greater anodization current of 100 mA/cm^2. The results of depositing indium into these modified PS samples are presented in Fig. 6.

It is evident from the results that increasing the lateral pore sizes by either removing the subsurface porous layer or increasing the anodization current density have no noticeable effect on the metal's

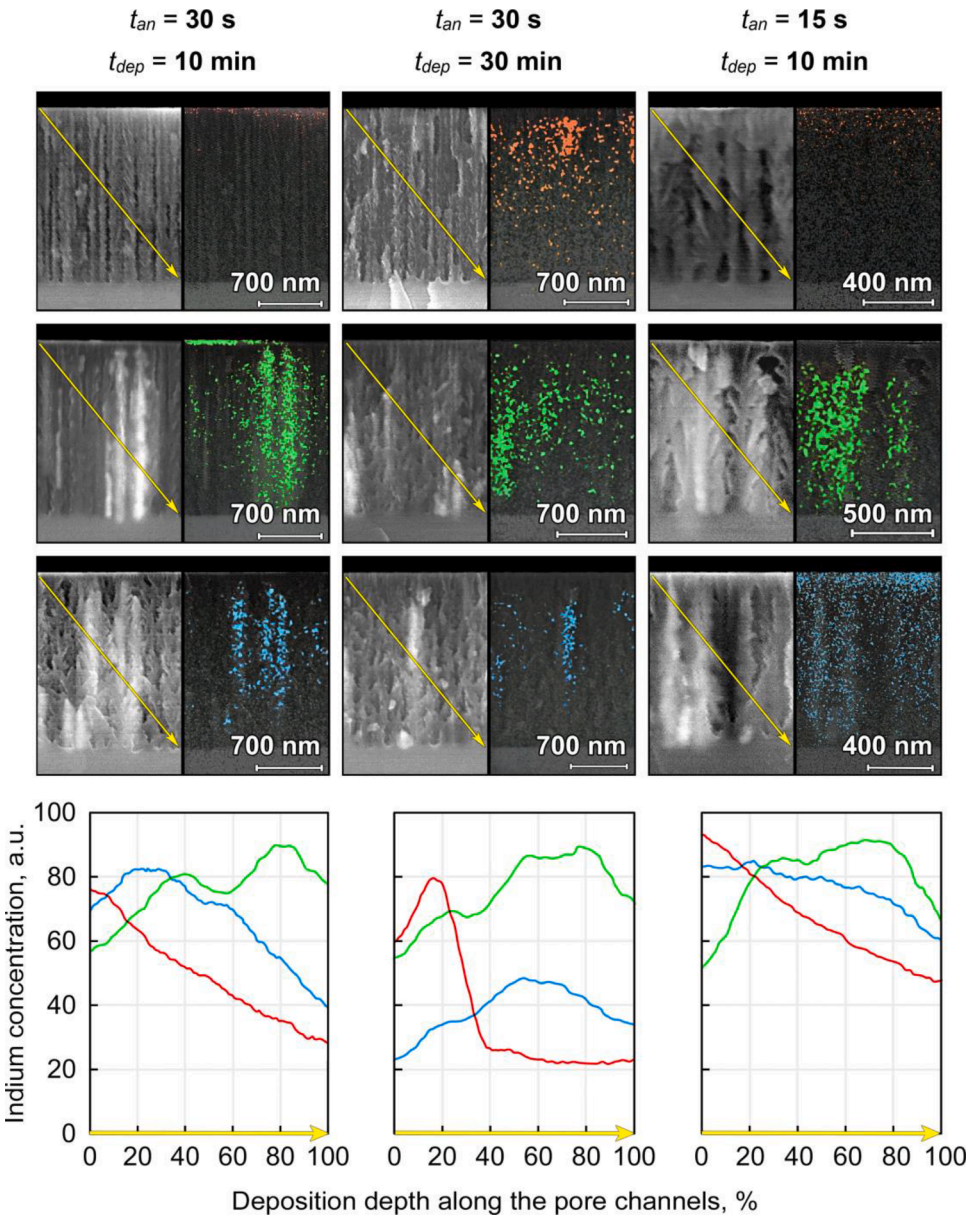

Fig. 3. Cross-section SEM images of indium-plated PS samples obtained at different anodization (t_{an}) and indium deposition (t_{dep}) times (left side of each image) after thermal treatment and corresponding EDS maps (right side) showcasing indium distribution (colored areas) and EDS-based concentration profiles of indium deposited into (red) unoxidized, (green) chemically oxidized and (blue) thermally oxidized PS layers of various thicknesses and subsequently annealed. Yellow arrows indicate the position and direction of EDS scans.

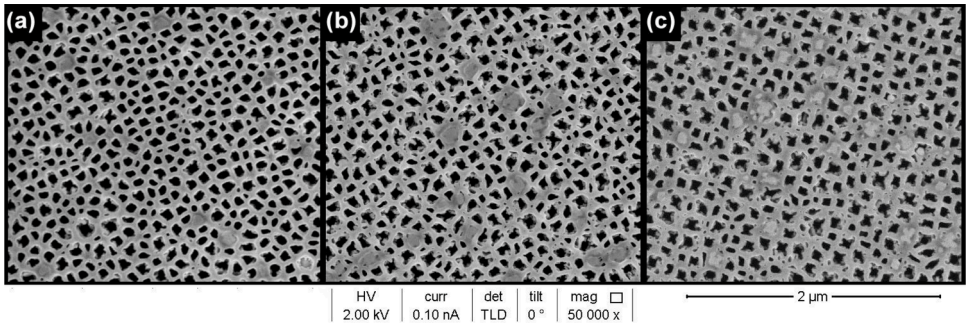

Fig. 4. Surface SEM images of (a) unoxidized, (b) chemically and (c) thermally oxidized PS samples plated with indium used for statistical analysis.

distribution, suggesting that a different mechanism is at play.

Another approach to increasing pore filling included indium deposition at a higher current density value of 5 mA/cm^2, which was attempted to increase the number of electrical breakdown points of SiO_2 layers on the pore sidewalls. Indium was also deposited into a porous silicon wafer that was not preliminarily exposed to the electrolyte for 30 min (unlike the rest of the samples presented above). Since the oxidation of pore sidewalls does not occur when negative voltage is applied in an acidic aqueous deposition solution, this approach allows to completely avoid oxidation by the solution itself and examine the deposition process

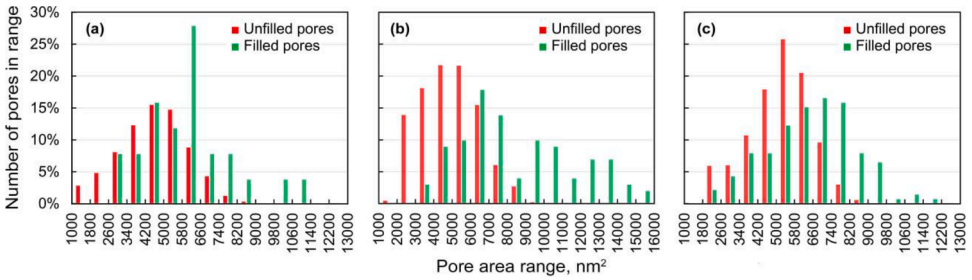

Fig. 5. Size distribution of empty and indium-filled pores obtained by electrochemical deposition of indium into (a) unoxidized, (b) chemically and (c) thermally oxidized PS.

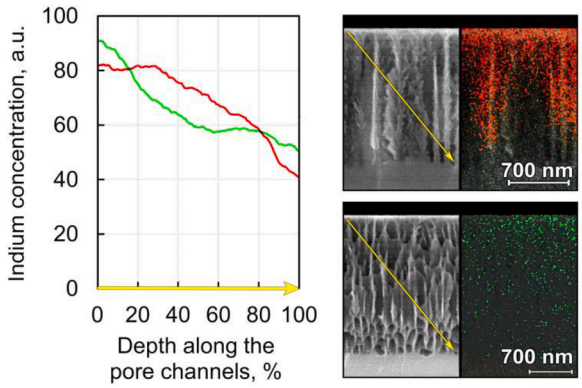

Fig. 6. EDS-based concentration profiles of indium distribution and cross-section SEM images of indium-plated PS samples with larger pore diameters: (red) indium in PS with its subsurface layer removed by ion sputtering; (green) indium in PS obtained at a higher anodization current density (100 mA/cm^2). Yellow arrows indicate the position and direction of EDS scans.

in the case of a completely unoxidized sample. The according results are compiled in Fig. 7.

Contrary to increasing the pore size, applying a greater deposition current value created a significantly larger number of filled pores, indicating an increased amount of nucleation points and additionally accentuating the conglomerates' formation in vertically-aligned cylindrical shapes.

4. Discussion

According to EDS data and SEM images of PS samples filled with indium prior to thermal treatment (Fig. 2), additional oxidation helps to improve metal deposition inside the porous structure and achieve its more uniform distribution along the pore channels. However, as the depth of the porous layer increases, the effect of oxidation gets noticeably reduced.

Annealing of unoxidized PS with indium particles causes the latter to shift towards the pores' subsurface areas or leave them altogether, whereas in the case of pre-oxidized samples indium continues to flow down the pores when exposed to high temperatures. It would seem that performing annealing on oxidized PS filled with indium allows to spread out the deposited material more evenly, shifting it slightly further down the pore channels and «connecting» the separated particles. The particles' overall spatial distribution, however, is not affected in any significant manner. The observed difference can be caused by increased wettability due to the formation of oxide on the pore sidewalls. Oxidized silicon is significantly more hydrophilic, which is reflected by the change in the contact angle of liquids to the surface of the wafer. To test the difference in wettability in this particular case, a 20 μl deposition solution droplet and a liquid indium droplet (preliminarily heated to 200 °C) were administered onto the surface of two samples: one unoxidized (with any residual SiO_2 prevalently removed in a 4.5% aqueous HF solution) and one oxidized in a 50% aqueous HNO_3 solution for 30 min. As the results presented in Fig. 8 would suggest, an about 55% decrease in contact angle is apparent after the surface is oxidized, both in the cases of the deposition solution droplet (47° to 21°) and the melted indium particle (135° to 60°), indicating a large difference in surface wettability that would also apply to the surface of the pore channels.

The heights of the forming cylindrical indium structures that are especially pronounced at higher deposition currents seem to grow smaller the deeper they are into the pore channels, which can most likely be attributed to various diffusion limitations. Presumably, the current flow is halted in the layer's uppermost areas because of their preferential oxidation, while the processing of the pore bottoms is slowed down due to the mass transfer being considerably restricted by the pores'

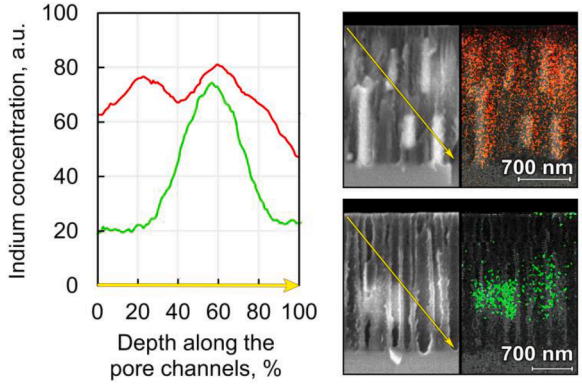

Fig. 7. EDS-based concentration profiles of indium distribution and cross-section SEM images of indium-plated PS samples with larger pore diameters: (red) indium deposited at a higher current density (5 mA/cm^2); (green) indium deposited into PS that wasn't preliminarily exposed to the deposition solution for 30 min. Yellow arrows indicate the position and direction of EDS scans.

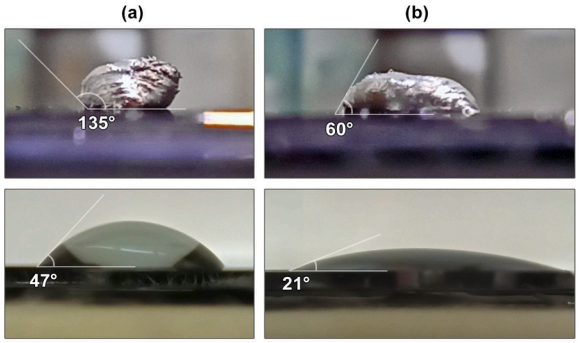

Fig. 8. Photographs of (top row) liquid indium and (bottom row) deposition solution droplets on the surfaces of (a) unoxidized and (b) chemically oxidized monocrystalline silicon illustrating the difference in surface wettability angles.

miniscule lateral sizes. Various factors can obstruct the reagent and byproduct diffusion into and out of the pore channels, including but not limited to the small lateral sizes of pores, large metal conglomerates accumulating near the pores' entrances, as well as the subsurface porous layer with smaller pore diameters.

Before external voltage is applied, the space charge region envelops the entirety of the porous layer [12]. Additionally, as the majority of the samples were immersed in the deposition solution for quite some time before the current was applied, a thin oxide layer most likely remained an important factor regardless of whether or not any additional oxidation was performed. We have hypothesized that the deposition process is initiated when a local breakdown of the dielectric layer consisting of oxidized silicon occurs, primarily on the points where the oxide layer is at its thinnest. Nucleation may also take place at various surface point defects such as antimony doping atoms, oxygen and hydrogen atoms, impurities and other absorbed species that locally lower the surface barrier and hence the breakdown voltage. Formation of initial indium nuclei on the surface of the pore leads to voltage redistribution. The surface can no longer be considered equipotential, and any further metal deposition only takes place on the already formed indium clusters. Restricted by the pore channels' shape, the resulting indium nuclei then continue to grow into cylindrical structures, provided that the current is maintained and the pore channels above are not clogged by other indium deposits, preventing the electrolyte's renewal. A generalized case of a process described above is presented in Fig. 9.

However, for a more accurate representation of the deposition process, porous layer thickness should also be considered, as it seems to play a major role in the distribution of indium, especially in the case of unoxidized samples. While the diffusion limitations present in thicker PS layers, as already mentioned, greatly add to this role, another possible reason may be the differences in resistivity of the silicon crystallites and its correlation with the resistivity of the deposition solution columns in the PS pores. Resistivity of the crystallites forming the PS matrix increases with pore depth, making deeper plating more favorable. (Fig. 10).

Additional oxidation of PS prior to depositing indium reduces the possibility of electrical breakdown at the surface, thus suppressing deposition there and making deeper plating more likely. However, it does not fully eliminate nucleation along the pore sidewalls. Preliminary oxide formation may also additionally assist the deposition process by increasing the wettability of the side walls and reducing the negative effect of diffusion limitations. In contrast to that, indium deposition in the case of a sample which was not kept in the deposition solution prior to electrochemical processing and is therefore completely unoxidized takes place at a certain depth inside of the PS layer (Fig. 7), but deposition soon halts due to the solution's eventual depletion, indicating that unoxidized pore sidewalls do not promote the supply of more electrolyte from the subsurface areas due to their limited wettability, further empathizing the importance of an additional oxidation stage.

In the cases of thick PS (about 10 μm deep), however, the increased resistivity of the silicon crystallites is similar to the effect of additional oxidation, making the latter less effective in controlling indium distribution, which manifests in concentration profiles grouping closer together as the thickness of the porous layer is increased (Fig. 2).

The idea of indium nucleation at the silicon oxide breakdown points is supported by the results of indium deposition at higher current densities (see Figs. 6 and 7). The number of oxide breakdown points increases with the deposition current density due to higher voltage being applied, which enables indium nucleation on thicker oxide layers. Mesoporous silicon's subsurface layer with smaller pore sizes attributes to the diffusion limitations, so removing it allows for easier deposition solution renewal inside the pores, positively affecting plating depth.

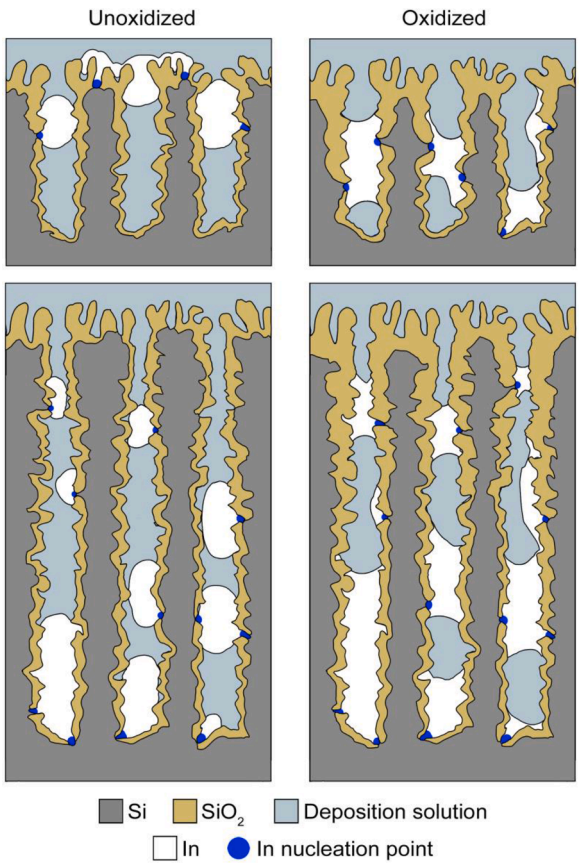

Fig. 10. Schematic illustration of the proposed indium nucleation and growth mechanism in the cases of utilizing unoxidized and preliminarily oxidized porous layers of different thicknesses.

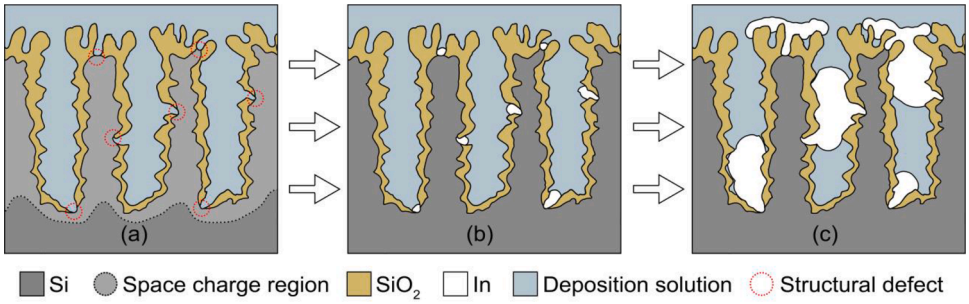

Fig. 9. Hypothetical stages of indium electrodeposition into PS: (a) initial porous layer prior to applying the current; (b) nucleation of indium particles at surface points where the oxide layer is thinnest after applying the current; (c) fully-grown indium structures along the pore channels and on the surface after deposition time elapses.

5. Conclusions

The results deriving from the EDS mapping data implicate that oxidation of PS samples prior to electrochemically depositing indium into their pores partially localizes the deposition process, making the metal particles reside closer to the bottoms of the pore channels. The highest indium concentrations have been achieved on samples oxidized chemically using HNO_3 and annealed post-deposition. However, oxidation becomes less effective as the thickness of the porous layer is increased due to the gradually escalating effect of reduced conductivity at the pore tips. Another way of slightly improving plating depth involves removing the PS's subsurface layer with lesser pore sizes, which can eliminate some of the diffusion limitations.

Additional short-time exposure to temperatures above indium's melting point causes the metal particles to redistribute throughout the pore channels depending on the selected oxidation regime. Namely, indium's concentration in unoxidized thermally-treated samples is smaller than that in their oxidized counterparts and decreases linearly with depth. In contrast to that, the metal's distribution throughout both chemically and thermally oxidized porous layers after their annealing is much more even, which is attributed to their higher wettability allowing the metal to shift further down the pore channels. Despite a slight shift down the pore channels, the overall effect of annealing on the metal's overall distribution for oxidized samples is not considered significant.

Non-uniform pore filling remains an issue, manifested in not each consecutive pore having indium deposits in it. While the initial analysis would implicate that the largest pores have a tendency to be filled first, increasing the pore size did not have any positive effect on the amount of pores filled, suggesting that a different unexplored mechanism is at play here. Of all the examined approaches, the only one to increase the amount of pores filled is increasing the deposition current density, which in turn creates more nucleation points by lowering the breakdown voltage of the oxide layer present on the pore sidewalls.

Presumably, PS layers with indium particles uniformly localized in the bottommost parts of the pore channels can be used as a base for the creation of germanium nanostructures and Si-Ge alloys using the *ec-LLS* process, where they simultaneously act as microscopic cathodes and a growth medium for crystalline germanium.

CRediT authorship contribution statement

Nikita Grevtsov: Methodology, Formal analysis, Investigation, Writing – original draft. **Eugene Chubenko:** Methodology, Validation, Supervision, Writing – review & editing. **Vitaly Bondarenko:** Conceptualization, Resources, Supervision, Project administration, Writing – review & editing. **Ilya Gavrilin:** Investigation, Resources. **Alexey Dronov:** Investigation. **Sergey Gavrilov:** Investigation, Funding acquisition.

Declaration of Competing Interest

The authors declare that they have no known competing financial interests or personal relationships that could have appeared to influence the work reported in this paper.

Acknowledgements

We thank D. Zhigulin (State Center "Belmicroanalysis", JSC "INTEGRAL", Minsk, Belarus), R. Volkov and N. Borgardt (Center of Shared Facilities "Diagnostics and modification of microstructures and nanoobjects", MIET, Zelenograd, Moscow, Russia) for performing SEM and EDS analysis of the experimental samples.

This research was financially supported by the Russian Science Foundation (Project no. 20-19-00720).

References

[1] P. Lobacarro, A. Raygani, A. Oriani, N. Miani, A. Piotto, R. Kapadia, M. Zheng, Z. Yu, L. Magagnin, D.C. Chrzan, R. Maboudian, A. Javey, Electrodeposition of high-purity indium thin films and its application to indium phosphide solar cell, J. Electrochem. Soc. 161 (2014) 794–800.

[2] G. Rakhymbay, M.K. Nauryzbayev, B.D. Burkitbayeva, A.M. Argimbaeva, R. Jumanova, A.P. Kurbatov, M. Eyraud, P. Knauth, F. Vacandio, Electrochemical deposition of indium: nucleation mode and diffusional limitation, Russ. J. Electrochem. 52 (2016) 99–105.

[3] C. Deferm, J.C. Malaquitas, B. Onghena, D. Banerjee, J. Luyten, H. Oosterhof, J. Fransaer, K. Binnermans, Electrodeposition of indium from the ionic liquid trihexyl(tetradecyl)phosphonium chloride, Green Chem. 21 (2019) 1517–1530.

[4] W. Monnens, C. Deferm, J. Sniekers, J. Fransaer, K. Binnermans, Electrodeposition of indium from non-aqueous electrolytes, Chem. Commun. 55 (2019) 4789–4792.

[5] S. Abdullah, M.R. Muhamad, K.A. Sekak, Effects of indium depositions on porous silicon nanostructure (PSN), Mater. Sci. Forum 517 (2006) 267–271.

[6] T. Ito, T. Yoneda, K. Furuta, A. Hatta, A. Hiraki, Improvement in visible luminescence properties of anodized porous silicon by indium plating, Jpn. J. Appl. Phys. 34 (1995) 649–652.

[7] J. DeMuth, E. Fahrenkrug, S. Maldonado, Controlling nucleation and crystal growth of Ge in a liquid metal solvent, Cryst. Growth Des. 16 (2016) 7130–7138.

[8] S. Acharya, L. Ma, S. Maldonado, Critical factors in the growth of hyperdoped germanium microwires by electrochemical liquid−liquid−solid method, ACS Appl. Nano Mater 1 (2018) 5553–5561.

[9] I. Gavrilin, D. Gromov, A. Dronov, S. Dubkov, R. Volkov, A. Trifonov, N. Borgardt, S. Gavrilov, Effect of electrolyte temperature on the cathodic deposition of Ge nanowires on in and Sn particles in aqueous solutions, Semiconductors 51 (2017) 1067–1071.

[10] E. Chubenko, S. Redko, A. Dolgiy, H. Bandarenka, S. Prischepa, V. Bondarenko, Porous silicon as host and template material for fabricating composites and hybrid materials, in: G. Korotcenkov (Ed.), Porous Silicon: From Formation to Application, CRC Press, Boca Raton, 2016, pp. 183–207.

[11] L. Canham, Handbook of Porous Silicon, Springer, 2018 second ed.Switzerland.

[12] E. Chubenko, S. Redko, A. Sherstnyov, V. Petrovich, D. Kotov, V. Bondarenko, Influence of the surface layer on the electrochemical deposition of metals and semiconductors into mesoporous silicon, Semiconductors 50 (2016) 372–376.